



Causal Evidence for the Primordality of Colors in Trans-Neptunian Objects

BENJAMIN L. DAVIS ^{1,*} MOHAMAD ALI-DIB ^{1,*} YUJIA ZHENG (郑雨嘉) ^{2,*} ZEHao JIN (金泽灏) ^{1,*}
KUN ZHANG (张坤) ^{2,3} AND ANDREA VALERIO MACCÌO ^{1,4}

¹*Center for Astrophysics and Space Science (CASS), New York University Abu Dhabi, PO Box 129188, Abu Dhabi, UAE*

²*Carnegie Mellon University, Pittsburgh, PA, USA*

³*Mohamed bin Zayed University of Artificial Intelligence, Abu Dhabi, UAE*

⁴*Max-Planck-Institut für Astronomie, Königstuhl 17, 69117 Heidelberg, Germany*

(Received April 4, 2025)

Submitted to AAS Journals

ABSTRACT

The origins of the colors of Trans-Neptunian Objects (TNOs) represent a crucial unresolved question, central to understanding the history of our Solar System. Recent observational surveys have revealed correlations between the eccentricity and inclination of TNOs and their colors. This has rekindled the long-standing debate on whether these colors reflect the conditions of TNO formation or their subsequent collisional evolution. In this study, we address this question with 98.7% certainty, using a model-agnostic, data-driven approach based on causal graphs. First, as a sanity check, we demonstrate how our model can replicate the currently accepted paradigms of TNOs’ dynamical history, blindly and without any orbital modeling or physics-based assumptions. We then show how this model predicts, with high certainty, that the color of TNOs is the root cause of their inclination distribution, rather than the other way around. This strongly suggests that the colors of TNOs reflect an underlying dynamical property, most likely their formation location. Moreover, our causal model excludes formation scenarios that invoke substantial color modification by subsequent irradiation. We therefore conclude that the colors of TNOs are predominantly primordial.

Keywords: Kuiper belt (893); Small Solar System bodies (1469); Trans-Neptunian objects (1705); Astrostatistics (1882)

1. INTRODUCTION

Trans-Neptunian Objects (TNOs) are invaluable probes into the history and evolution of our Solar System (A. Morbidelli & D. Nesvorný 2020). However, the wealth of information they encode is often difficult to decipher. This includes intrinsic characteristics such as their sizes and correlated properties such as their orbits and surface photometric colors. The last two have long been closely examined in an effort to unravel the relation between them (D. C. Jewitt & J. X. Luu 2001).

Although the history of these studies is long, here we focus on M. Marsset et al. (2019) who found a strong correlation between the inclination and colors of TNOs.

More precisely, using the Colours of the Outer Solar System Origin Survey (COI-OSSOS; M. E. Schwamb et al. 2019) observations, they concluded that Very Red Objects (VROs) have a cutoff maximum inclination of around 21°, in contrast to the more gray Less Red Objects (LROs). These results were expanded by M. Ali-Dib et al. (2021), who found an analogous trend where the eccentricity of VROs is cutoff at 0.42. They concluded that there is a paucity of VROs in the scattered disk, and used a Solar System formation model to explain these trends as a consequence of their formation location in the disk. In this scenario, using causality theory jargon, eccentricity (e) and inclination (i) are said to be caused by the colors, which is indicative of the formation location.

The primordial origin hypothesis of the TNO color diversity argues that TNO colors reflect compositional

Email: ben.davis@nyu.edu

* These authors contributed equally to this work and are listed alphabetically.

gradients in the protoplanetary disk, preserved since formation (D. Nesvorný et al. 2020; M. Ali-Dib et al. 2021). Objects formed at different heliocentric distances thus acquired distinct volatile and refractory compositions, leading to color variations. For example, objects that formed beyond the CO and N₂ snowlines could have acquired redder surfaces. Dynamical processes (e.g., planetary migration and scattering) later redistributed these bodies into their current orbits, imprinting correlations between color and orbital parameters like inclination.

However, in an alternative way, many works (J. X. Luu & D. C. Jewitt 1996; S. A. Stern 2002) argued that collisional evolution is the origin of TNO colors, where collisions expose fresh subsurface ices or organic materials, altering albedo and spectral slopes. Dynamically excited populations (higher e and i) experience more frequent collisions due to orbital crossings, leading to color–inclination correlations. This framework treats color as a secondary property shaped by post-formation bombardment. Opponents of this model argue that if collisional resurfacing were causal, dynamically excited populations would exhibit homogenized colors over time due to frequent mixing.

A third possibility proposed that initially diverse bulk compositions undergo selective volatile evaporation post-formation, establishing steep compositional gradients across the primordial disk that, coupled with subsequent UV photolysis and particle irradiation, yield distinct surface chemistries (M. E. Brown et al. 2011; I. Wong & M. E. Brown 2017). A key difference between this and the “primordial origin” hypothesis is the necessity of post-formation irradiation. From a causality lens, this introduces a causal relationship between the current semimajor axis and the color of TNOs.

In this Letter, we use a purely data-driven, model-agnostic, statistical causal discovery method to study the relationships between the dynamical parameters of TNOs, and between those and the TNO colors. We show that not only this technique allows us to derive some of the main lines of the current consensus on the origins of TNOs, but also that it elucidates the direction of causality between the dynamical parameters and colors of TNOs. We first detail an overview of our causal discovery methods (§2) including a description of our data sample (§2.1), present the results of our analysis (§3), and conclude with a discussion and overall summary (§4). Additionally, we include an Appendix (§A) to cover the details of our ancillary test with Gaussianization.

2. METHODOLOGY

2.1. Data

Our dataset is based on (but not exclusively) the Col-OSSOS survey (M. E. Schwamb et al. 2019). It was taken from M. Marsset et al. (2019) and M. Ali-Dib et al. (2021). It consists of a total of 229 TNOs including hot classicals, centaurs, and resonant/scattered objects, in a dataset for which discovery biases were modeled. For each TNO, we have three orbital elements: semimajor axis (a), eccentricity (e), and inclination (i); and we have spectral slope (i.e., color).

A fundamental assumption of this work is that colors are primordial, and thus strongly correlated to the initial location of a TNO. Hereafter, we treat colors as a proxy for the initial semimajor axis of the objects. See Fig. 1 for a pairplot showing all the pairwise relations between our data.⁵ Additionally, Fig. 1 shows the subpopulation in our data by separating each TNO by its classifications as either a Classical (48), Resonant (102), Centaur (36), Scattered (28), or Detached (15) object.

Our dataset is further summarized in Fig. 2. We define VROs as TNOs with spectral slopes greater than 20.6%/(10³ Å). The color–eccentricity correlation is revealed in this plot as a paucity of VROs for eccentricity above 0.42. Similarly, the color–inclination correlation manifests itself as a lack of VROs for inclinations above 21°.

2.2. Causal Discovery: Identifying Cause-effect Relationships

Identifying cause-effect relationships is crucial for moving beyond mere correlation to uncover the underlying causal mechanisms governing a system. Traditionally, causal relationships are established through interventions or randomized experiments, where one variable is explicitly manipulated while all others are held constant, and the resulting effects are observed. However, such interventions are infeasible in fields like astronomy, where the “test subjects” exist at unreachable astronomical distances. Consequently, advanced methods are required to infer causal relationships from purely observational data—an endeavor that lies at the core of causal discovery (P. Spirtes et al. 2001).

The foundation of causal discovery lies in uncovering the footprints of causality embedded in data. One of the most important sources of such information is dependency relations. By analyzing conditional independence among different components of an observed sys-

⁵ See §A for a further test on applying nonlinear transformations to Gaussianize our data.

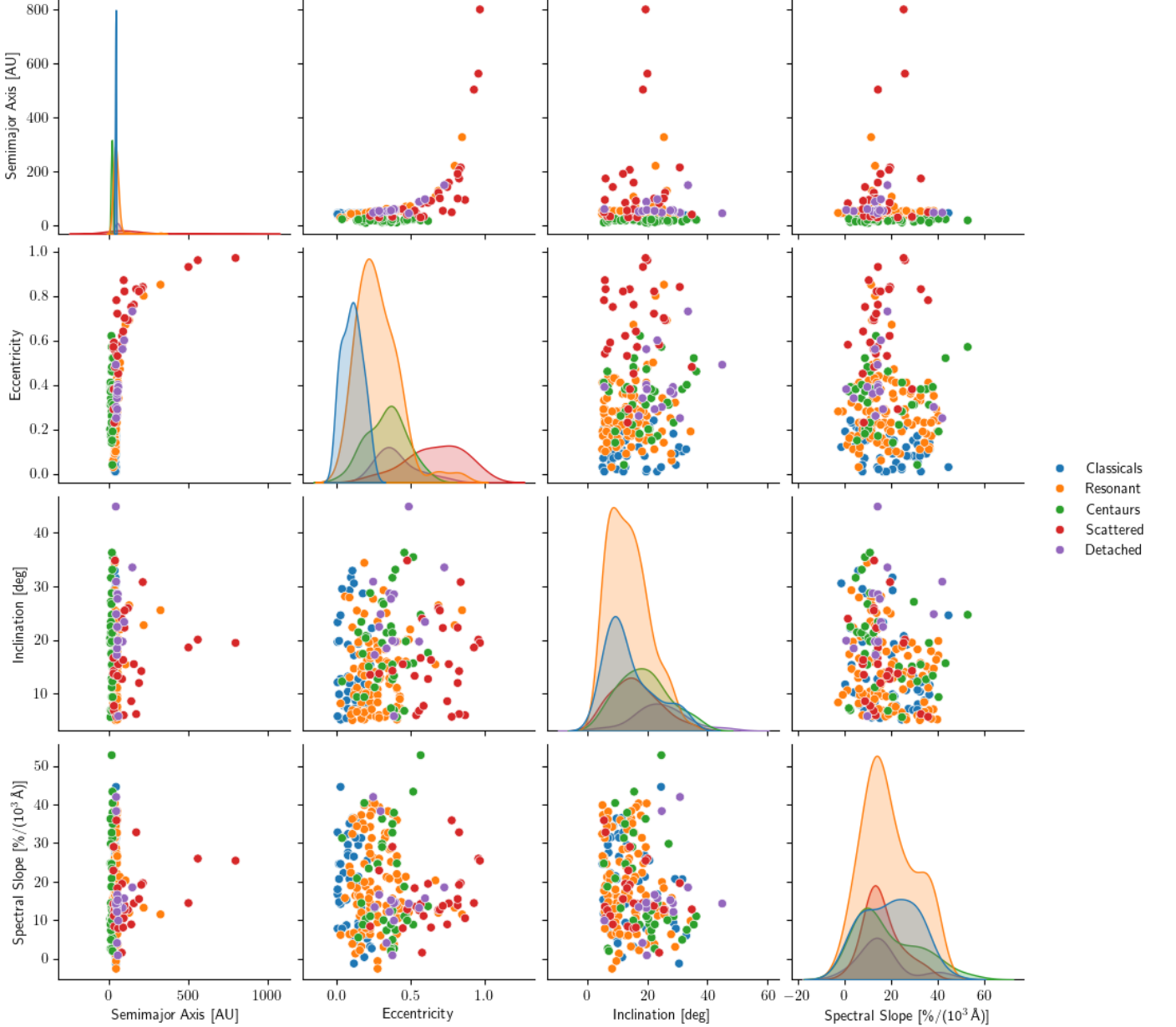


Figure 1. Pairplot of all 229 TNOs in our study. The TNOs are further divided into their individual populations: 48 Classicals (●), 102 Resonant (●), 36 Centaurs (●), 28 Scattered (●), and 15 Detached (●).

tem, we can infer causal relationships between pairs of variables. This allows us to construct a graph that encodes the results of essential conditional independence tests, revealing which variables *cause* others under appropriate conditions. Ideally, the output is a Directed Acyclic Graph (DAG) for a unique solution or a Completed Partially Directed Acyclic Graph (CPDAG) for a Markov equivalence class. However, when some variables remain unmeasured, certain causal relationships may be undetermined, leading to a Partial Ancestral Graph (PAG). For further reading on causal discovery and causality, see *Causation, Prediction, and Search* (P.

Spirtes et al. 2001), *Causality* (J. Pearl 2009), or the review in Z. Jin et al. (2025b, §2).⁶

2.3. Causal Structures with Latent Variables

Since it is impossible to measure all variables in the Universe, latent variables are always present. These unmeasured variables can significantly impact the correctness of the causal structure discovered. For example,

⁶ In addition to Z. Jin et al. (2025b), readers may be interested in further applications of causal discovery to astrophysical data (M. Pasquato et al. 2023; M. Pasquato 2024; Z. Jin et al. 2024, 2025a).

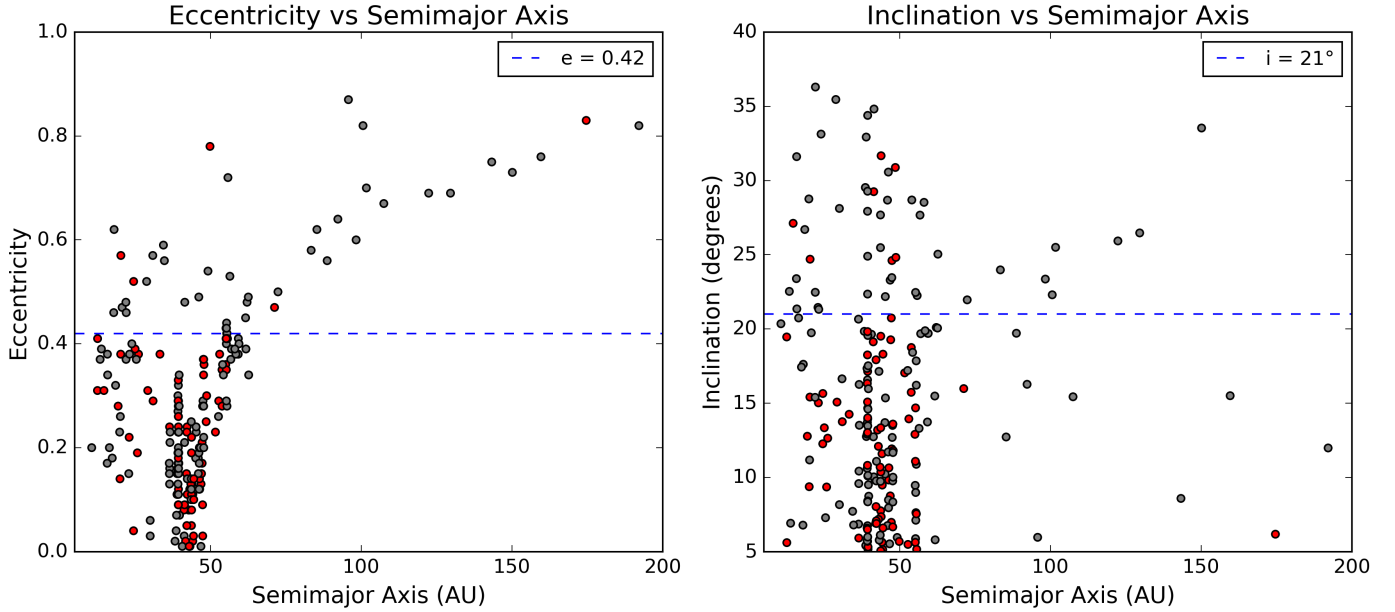


Figure 2. The M. Marsset et al. (2019) and M. Ali-Dib et al. (2021) sample shown as $a-e$ (left) and $a-i$ (right) plots. Colors were defined such that red (●) is for Very Red Objects (spectral slopes higher than $20.6\%/(10^3 \text{ \AA})$) and gray (●) is for Less Red Objects. The plot clearly shows the paucity of VROs for eccentricities higher than 0.42 and inclinations higher than 21° , respectively (---).

suppose that X and Y are independent in the general population, but a sample is selected based on a variable Z that influences both X and Y . In that case, X and Y may exhibit statistical dependence in the sample, even though no such relationship exists in the population. This can lead to spurious causal conclusions, falsely suggesting a direct causal relationship between X and Y .

To address this challenge, we employ a principled approach capable of uncovering causal relationships even in the presence of latent variables. A widely used method for this purpose is Fast Causal Inference (FCI; P. Spirtes et al. 1995; J. Zhang 2008), a constraint-based algorithm that has been proven to provide sound causal conclusions despite unmeasured variables. FCI has been applied across various scientific domains, including biology, economics, and climate science. For our analysis of TNO orbits, we use the FCI implementation in the Python package `causal-learn` (Y. Zheng et al. 2024) to infer the underlying causal structure.

FCI discovers causal relationships by performing a series of conditional independence (CI) tests. These tests examine whether the statistical dependence between two variables disappears when controlling for other variables. If two variables become independent when conditioning on a third, this suggests that the third variable may be an intermediary or a common cause.

Unlike many causal discovery methods that assume that all relevant variables are measured (such as those

producing DAGs or CPDAGs), FCI accounts for the possibility of unobserved variables. As a result, its output is a PAG, which provides more nuanced causal information. The edges in a PAG have different interpretations:

- $X \longrightarrow Y$: X is a *cause* of Y .
- $X \circ \longrightarrow Y$: Y is not an *ancestor* of X . Intuitively, this implies Y cannot be a cause of X , whether directly or indirectly.
- $X \circ - \circ Y$: No set d -separates X and Y . In other words, they may be causally adjacent or share a latent common cause.
- $X \longleftrightarrow Y$: There is a latent common cause of X and Y .

Therefore, by accounting for latent variables in the discovery process, we can uncover causal relations among measured variables while acknowledging uncertainties introduced by unmeasured factors. More importantly, when the algorithm cannot determine a definitive causal direction due to latent variables, it explicitly represents this uncertainty rather than arbitrarily assigning a direction. This principled approach distinguishes causal analysis from correlation-based techniques, ensuring that conclusions are drawn with a clear acknowledgment of underlying assumptions and limitations.

3. RESULTS

3.1. Data-driven Results

Our primary findings are summarized in Fig. 3 showing the statistically most likely PAG fitting our data, at 98.7% confidence. This main result utilizes the FCI algorithm (P. Spirtes 2001; P. L. Spirtes et al. 2013; Y. Zheng et al. 2024), with linear Fisher-Z conditional independence tests (R. A. Fisher 1921), and the threshold for each conditional independence test is $\alpha = 0.013$ (i.e., all tests must pass at the 98.7% level) on transformed data via Gaussianization. The motivation and details of the Gaussian transformation can be found in §A. We still get the same PAG using a linear Fisher-Z test without any transformation for $\alpha = 0.02$. It is also possible to directly use a non-linear conditional independence test. Here, we adopt a Kernel-based conditional independence (KCI) test (K. Zhang et al. 2012), with a polynomial kernel and reproduce the same PAG as in Fig. 3 at $\alpha = 0.09$.⁷

We emphasize that this PAG was obtained with a purely data-driven approach, without astrophysical insights. Moreover, we consistently reproduce the same PAG as in Fig. 3 by jackknifing our data by sequentially leaving out each subpopulation of TNOs. Thus, removing any subsample of 48 Classicals, 102 Resonant, 36 Centaurs, 28 Scattered, or 15 Detached TNOs results in no change to our discovered PAG. Therefore, we demonstrate that no single subpopulation is dominating the PAG and that our results are robust to outliers.

Alternatively, if we are to generate PAGs for the individual populations separately (i.e., analyzing only one subpopulation at a time), we find a large diversity in the results. Many of these PAGs however are based on very few datapoints. Taking this result at face value hints that our overall PAG represents that main-line dynamics dominate over the entire sample.

3.2. Astrophysical Interpretation

The first link we investigate is the one-way causal direction of the *current* semimajor axis causing the *current* eccentricity. While the correlation between a and e in TNOs is well established, the direction of the causality we find here is not surprising either, as its root physical causes are:

- Scattering by Neptune, where objects have to close-encounter Neptune first in order to get scattered into high eccentricity orbits. Moreover, ob-

⁷ We did not apply non-linear tests in the first place because a non-linear method is prone to overfitting for the relatively small size of our data (229 TNOs).

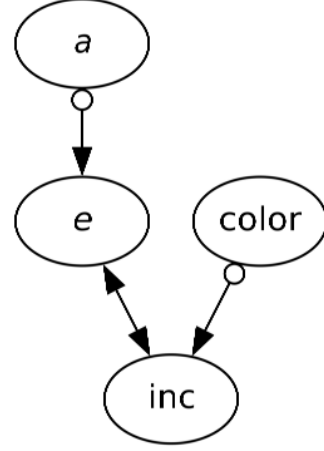


Figure 3. Partial Ancestral Graph (PAG) for 229 TNOs, calculated with the Fast Causal Inference (FCI) algorithm (P. Spirtes 2001; P. L. Spirtes et al. 2013; Y. Zheng et al. 2024), for linear Fisher-Z conditional independence tests (R. A. Fisher 1921) on transformed data, with $\alpha = 0.013$ (significance level of individual partial correlation tests). On untransformed data, we recover the identical PAG with linear Fisher-Z tests and $\alpha = 0.02$, while the same PAG is produced with $\alpha = 0.09$ when we run Kernel-based conditional independence (KCI) tests (K. Zhang et al. 2012), with a polynomial kernel. This PAG has three causal edges, which can be described as follows: (i) eccentricity is not an ancestor of the semimajor axis, (ii) there is a latent common cause of eccentricity and inclination, and (iii) inclination is not an ancestor of color.

jects usually cannot be both close to Neptune (today) and have a high eccentricity. It is the current semimajor axis of the objects that dictates what eccentricity they can have, and not the other way around.

- Mean motion resonances (MMRs), where the period (and thus current semimajor axis) of the objects dictates whether they are inside an eccentricity-raising resonance.

The connection $a \rightarrow e$ rules out the possibility of $a \leftarrow e$. Clearly, $a \rightarrow e$ is possible, but also $a \leftrightarrow e$. The latter might imply that an unobserved confounder causes both a and e .

The second link in the PAG is the two-way dependency between the eccentricity and the inclination, which is consistent with the von Zeipel-Lidov-Kozai (H. von Zeipel 1910; M. L. Lidov 1962; Y. Kozai 1962) anti-correlated oscillations between these two quantities (both inside and outside of MMRs), that plays a central role in the dynamics of TNOs. Here, $e \leftrightarrow i$ implies that there is an unobserved confounder. Indeed, the von Zeipel-Lidov-Kozai mechanism involves perturba-

tions from a third body, here being Neptune. Together, the first two links successfully reestablish the main dynamical processes shaping the Kuiper belt (scattering, MMRs, and von Zeipel-Lidov-Kozai oscillations) without any physical inputs.

Finally, **the third piece** of the puzzle is the connection $\text{color} \rightarrow i$ *ruling out* the possibility of $\text{color} \leftarrow i$. The “color” (i.e., a proxy for the formation location in our null hypothesis) is hence causing the inclination. This is again dynamically expected, as the formation location relative to inclination-raising secular resonances such as f_7 and f_8 will strongly affect the inclination distribution of TNOs (C. D. Murray & S. F. Dermott 1999). Note that this link, however, leaves open the possibility of an unobserved confounder causing both color and the inclination. This confounder can be the formation location itself, if we were to assume the color and initial location to be two distinct variables instead of the color being a proxy for location.

Our result, that $\text{color} \leftarrow i$ is not allowed, rules out the model of J. X. Luu & D. C. Jewitt (1996) and S. A. Stern (2002), where collisional evolution shapes the colors of TNOs. Moreover, our result that $\text{color} \leftarrow a$ is not allowed either, rules out the model of M. E. Brown et al. (2011) and I. Wong & M. E. Brown (2017), where a would control the amount of irradiation a TNO is subjected to. We are hence left only with the “primordial origins” model where **the color is set entirely by the chemical composition of the formation location**.

Some further interesting features are found in the PAG:

- **The lack of correlation between the color and semimajor axis.** This is dynamically expected as all TNOs in our sample underwent dynamical interactions with Neptune, that tend to be chaotic in nature. For example, many of the relevant processes (scattering, resonances, etc.) depend on the phase angle at which the TNO encounters Neptune. Some examples of the chaotic outcomes of the TNO dynamics are shown in Figs. 11 and 12 of M. Ali-Dib et al. (2021). See also Fig. 3 of D. Nesvorný et al. (2016).
- **The indirect causation between the color (initial location) and the eccentricity through the inclination.** Taken at face value, this would indicate that while the initial location directly causes the inclination, it is the final semimajor axis that causes the eccentricity. The effect of the initial semimajor axis on the eccentricity is indirect, and happens through von Zeipel-Lidov-Kozai oscillations starting from high inclinations.

In all cases, we note that the correlation coefficient between the color and eccentricity is around 0.1, allowing for a minor correlation between the two that can be seen in less probable PAGs.

4. DISCUSSION & CONCLUSIONS

This work endeavors to resolve the tension between theories of primordial origins vs. subsequent evolution to account for the observed dispersion and correlations in TNO colors, a subject of a long debate. Our causal graph analysis, derived from a model-agnostic causal discovery framework, strongly favors the primordial origin hypothesis, with 98.7% certainty that *TNO color is causally antecedent to inclination, not a consequence of it*. While impacts undoubtedly modify surfaces, our results suggest they are not the dominant driver of color diversity. Moreover, our model seems to exclude any effects from the current semimajor axis on the color of TNOs, disfavoring models where continuous irradiation plays a large role in shaping the colors. This will be explored further in the future.

While many earlier works tried to explain the inclination–color and eccentricity–color correlations both separately and simultaneously, our causal approach isolates inclination as the key dynamical variable causally linked to color. This hints at a larger role for inclination-raising secular resonances in the very early Solar System. Indeed, M. Ali-Dib et al. (2021) proposed that the origins of the paucity of VROs in the scattered disk is strongly linked to the f_7 , and f_8 inclination modes. In this scenario, the color–eccentricity correlation is largely (although not necessarily entirely) a consequence of the more fundamental inclination–color correlation, where the two can be linked via the von Zeipel-Lidov-Kozai mechanism. This is consistent with the numerical model of M. Ali-Dib et al. (2021) who proposed von Zeipel-Lidov-Kozai oscillations as a transport vehicle for VROs between high inclination and high eccentricity regimes.

Finally, this work is a proof of principle for the use of causality models in planetary sciences. With large datasets ranging from asteroids to exoplanets, many discoveries await.

ACKNOWLEDGMENTS

This material is based on work supported by Tamkeen under the NYU Abu Dhabi Research Institute grant CASS. This research has made use of NASA’s Astrophysics Data System Bibliographic Services. YZ and KZ are supported by NSF Award No. 2229881, AI Institute for Societal Decision Making, NIH R01HL159805,

and grants from Quris AI, Florin Court Capital, and MBZUAI-WIS Joint Program. This research was carried out on the high-performance computing resources at New York University Abu Dhabi. The data and code used for this work are available for download from the following GitHub repository: <https://github.com/ZehaoJin/causalTNOs>.

Software: `causal-learn` (Y. Zheng et al. 2024), `Matplotlib` (J. D. Hunter 2007), `NetworkX` (A. A. Hagberg et al. 2008), `NumPy` (C. R. Harris et al. 2020), `Pandas` (W. McKinney 2010), `pgmpy` (A. Ankan & A. Panda 2015), `PyGraphviz`, `Python` (G. Van Rossum & F. L. Drake 2009), `SciPy` (P. Virtanen et al. 2020), `seaborn` (M. L. Waskom 2021)

ORCID IDS

Benjamin L. Davis 
<https://orcid.org/0000-0002-4306-5950>
 Mohamad Ali-Dib 
<https://orcid.org/0000-0002-6633-376X>
 Yujia Zheng (郑雨嘉) 
<https://orcid.org/0009-0003-5225-6366>
 Zehao Jin (金泽灏) 
<https://orcid.org/0009-0000-2506-6645>
 Kun Zhang (张坤) 
<https://orcid.org/0000-0002-0738-9958>
 Andrea Valerio Macciò 
<https://orcid.org/0000-0002-8171-6507>

APPENDIX

A. DATA PREPROCESSING

Since the Fisher Z-test used in our causal discovery algorithm assumes linear Gaussian distributions of the model, we apply deterministic, variable-wise transformations to our data for preprocessing. Specifically, we employ the Yeo-Johnson transformations (I. Yeo & R. A. Johnson 2000) as our primary preprocessing. For the semimajor axis (a) and eccentricity (e), we employ a combination of Yeo-Johnson and tanh-type transformations to better handle their nonlinear relationships. For inclination and spectral slope, the standard Yeo-Johnson Gaussianization is sufficient. As these transformations act independently on each variable and are deterministic, they preserve the underlying causal structure.

The proprocessed data for all 229 TNOs is displayed as a pairplot in Fig. 4. Using preprocessed data, we reproduce the same PAG structure as shown in Fig. 3 with $\alpha = 0.013$. Visual inspection of the transformed data confirms the effect of the transformation, making the data more suitable for the Fisher Z-test. The transformed scatter plots also provide insights into causal directions. For instance, when examining the relationship between spectral slope and inclination in the direction of spectral slope causing inclination (i.e., a linear model of $i = k \cdot \text{slope} + \epsilon$), the noise term ϵ appears more independent compared to the reverse direction, supporting this causal orientation in our final PAG.

REFERENCES

- Ali-Dib, M., Marsset, M., Wong, W.-C., & Dbouk, R. 2021, *AJ*, 162, 19
- Ankan, A., & Panda, A. 2015, in Proceedings of the 14th Python in Science Conference, ed. Kathryn Huff & James Bergstra, 6 – 11
- Brown, M. E., Schaller, E. L., & Fraser, W. C. 2011, *ApJL*, 739, L60
- Fisher, R. A. 1921, *Metron*, 1, 3–32
- Hagberg, A. A., Schult, D. A., & Swart, P. J. 2008, in Proceedings of the 7th Python in Science Conference, ed. G. Varoquaux, T. Vaught, & J. Millman, Pasadena, CA USA, 11 – 15
- Harris, C. R., Millman, K. J., van der Walt, S. J., et al. 2020, *Nature*, 585, 357–362
- Hunter, J. D. 2007, *Computing in Science & Engineering*, 9, 90–95
- Jewitt, D. C., & Luu, J. X. 2001, *AJ*, 122, 2099
- Jin, Z., Pasquato, M., Davis, B., Maccio, A., & Hezaveh, Y. 2025a, in American Astronomical Society Meeting Abstracts, Vol. 245, American Astronomical Society Meeting Abstracts, 120.03D
- Jin, Z., Pasquato, M., Davis, B. L., Macciò, A. V., & Hezaveh, Y. 2024, *arXiv e-prints*, [arXiv:2410.14775](https://arxiv.org/abs/2410.14775)
- Jin, Z., Pasquato, M., Davis, B. L., et al. 2025b, *ApJ*, 979, 212
- Kozai, Y. 1962, *AJ*, 67, 591
- Lidov, M. L. 1962, *Planet. Space Sci.*, 9, 719
- Luu, J. X., & Jewitt, D. C. 1996, *AJ*, 112, 2310

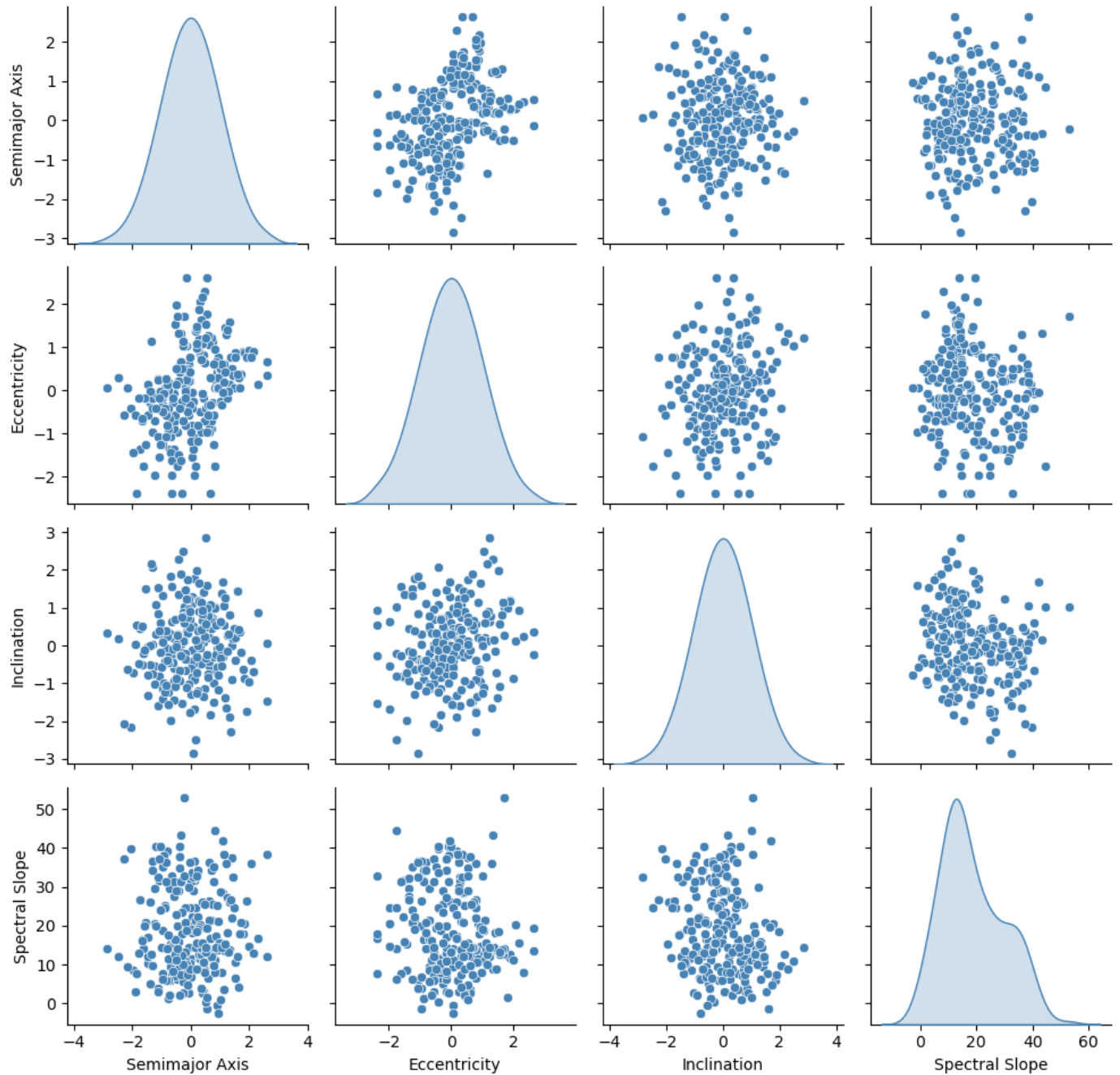


Figure 4. Pairplot of all 229 TNOs in our study that is similar to Fig. 1, except we have performed deterministic, variable-wise transformations to preprocess the data for the Fisher-Z test.

Marsset, M., Fraser, W. C., Pike, R. E., et al. 2019, [AJ](#), 157, 94

McKinney, W. 2010, in Proceedings of the 9th Python in Science Conference, Vol. 445, Austin, TX, 51–56

Morbidelli, A., & Nesvorný, D. 2020, in The Trans-Neptunian Solar System, ed. D. Pralnik, M. A. Barucci, & L. Young, 25–59

Murray, C. D., & Dermott, S. F. 1999, Solar System Dynamics

Nesvorný, D., Vokrouhlický, D., & Roig, F. 2016, [ApJL](#), 827, L35

Nesvorný, D., Vokrouhlický, D., Alexandersen, M., et al. 2020, [AJ](#), 160, 46

Pasquato, M. 2024, in EAS2024, European Astronomical Society Annual Meeting, 362

- Pasquato, M., Jin, Z., Lemos, P., Davis, B. L., & Macciò, A. V. 2023, [arXiv e-prints](#), [arXiv:2311.15160](#)
- Pearl, J. 2009, *Causality* (Cambridge university press)
- Schwamb, M. E., Fraser, W. C., Bannister, M. T., et al. 2019, [ApJS](#), **243**, 12
- Spirtes, P. 2001, in *Proceedings of Machine Learning Research*, Vol. R3, *Proceedings of the Eighth International Workshop on Artificial Intelligence and Statistics*, ed. T. S. Richardson & T. S. Jaakkola (PMLR), 278–285.
<https://proceedings.mlr.press/r3/spirtes01a.html>
- Spirtes, P., Glymour, C., & Scheines, R. 2001, *Causation, Prediction, and Search* (The MIT Press)
- Spirtes, P., Meek, C., & Richardson, T. 1995, in *Proceedings of the Eleventh Conference on Uncertainty in Artificial Intelligence*, 499–506
- Spirtes, P. L., Meek, C., & Richardson, T. S. 2013, [arXiv e-prints](#), [arXiv:1302.4983](#)
- Stern, S. A. 2002, [AJ](#), **124**, 2297
- Van Rossum, G., & Drake, F. L. 2009, *Python 3 Reference Manual* (Scotts Valley, CA: CreateSpace)
- Virtanen, P., Gommers, R., Oliphant, T. E., et al. 2020, [Nature Methods](#), **17**, 261
- von Zeipel, H. 1910, [Astronomische Nachrichten](#), **183**, 345
- Waskom, M. L. 2021, [Journal of Open Source Software](#), **6**, 3021
- Wong, I., & Brown, M. E. 2017, [AJ](#), **153**, 145
- Yeo, I., & Johnson, R. A. 2000, [Biometrika](#), **87**, 954–959
- Zhang, J. 2008, *Artificial Intelligence*, **172**, 1873–1896
- Zhang, K., Peters, J., Janzing, D., & Schoelkopf, B. 2012, [arXiv e-prints](#), [arXiv:1202.3775](#)
- Zheng, Y., Huang, B., Chen, W., et al. 2024, *Journal of Machine Learning Research*, **25**, 1–8